JULY 2016

SAN FRANCISCO ESTUARY & WATERSHED SCIENCE

Sponsored by the Delta Science Program and the UC Davis John Muir Institute of the Environment

RESEARCH

3-D Simulations of the San Francisco Estuary with Subgrid Bathymetry to Explore Long-Term Trends in Salinity Distribution and Fish Abundance

Michael L. MacWilliams*[1], Aaron J. Bever[1], and Erin Foresman[2]

Volume 14, Issue 2 | Article 3
doi: http://dx.doi.org/10.15447/sfews.2016v14iss2art3

* Corresponding author: mmacwilliams@anchorqea.com
1 Anchor QEA, LLC
San Francisco, CA 94111 USA
2 U.S. Environmental Protection Agency
San Francisco, CA 94105 USA

ABSTRACT

The UnTRIM hydrodynamic model was applied to San Francisco Bay and the Sacramento–San Joaquin Delta (Delta) using a coarse-resolution model grid with bathymetry represented at a finer subgrid scale. We simulated a 35-year period, spanning from January 1, 1980 through December 31, 2014. This simulation was used to develop salinity distribution maps to facilitate visualization of fish distribution and abundance data. We compared predicted salinity from the coarse-grid UnTRIM Bay–Delta model to continuous salinity monitoring observations as well to the measured surface salinity from San Pablo Bay through the Delta at a total of 5,542 times and locations where surface salinity was observed as part of several long-term fish monitoring programs: the Fall Midwater Trawl, Summer Townet Survey, and San Francisco Bay Study. The coarse-grid UnTRIM Bay–Delta model was shown to accurately predict hydrodynamics and the spatial distribution of salinity over both a 3-year detailed validation period and over the full 35-year analysis period. The predicted salinity was used to calculate the daily position of X2 and the daily-averaged area of the Low Salinity Zone (LSZ) for each day during the 35-year simulation. Our analysis highlights the influence of multi-year climate patterns, shorter-duration weather patterns, and Delta outflow on salinity distribution. We used the predicted salinity to develop maps of salinity distribution over seven periods for six fish species, and combined the salinity maps with historic fish sampling data to allow for visualization of fish abundance and distribution for 33 years between 1980 and 2012. These maps can be used to explore how different species respond to annual differences in salinity distributions in the San Francisco Estuary, and to expand the understanding of the relationships among salinity and fish abundance, distribution, and population resiliency.

KEY WORDS

San Francisco Bay, Hydrodynamic Modeling, UnTRIM, Low Salinity Zone, Fall Midwater Trawl, Bay Study, Fish Abundance, X2

INTRODUCTION

Long-term fisheries monitoring programs provide a valuable resource for understanding trends in fish abundance and distribution. These long-term monitoring programs in locations such as San

Francisco Bay (Baxter et al. 1999; Stevens and Miller 1983; CDFW 2015), and the Chesapeake Bay (MDNR 2015; VIMS 2015) have produced fisheries observations that now span multiple decades. Recent advances in computational resources and hydrodynamic models have made it possible to simulate hydrodynamics and salinity over the full span of these monitoring programs. Since detailed hydrodynamic models already exist for many estuaries, including both the San Francisco Estuary (estuary) (Chua and Fringer 2011; MacWilliams et al. 2015) and other estuaries such as Chesapeake Bay (Lanerolle et al. 2009, 2011; Xu et al. 2012), there is a significant opportunity to apply these models to improve our understanding of how long-term trends in salinity and other variables have influenced fish distribution and abundance over time. While variation in fish distribution relative to salinity and turbidity are well documented (e.g., Turner and Chadwick 1972; Moyle et al. 1992; Baxter et al. 1999; Sweetnam 1999; Feyrer et al. 2007; Rosenfield and Baxter 2007; Kimmerer et al. 2009; Bever et al. 2016), the availability of long-term continuous monitoring data for salinity, turbidity, and other variables that is needed to evaluate the effect of long-term trends is significantly more sparse toward the beginning of the fish monitoring data sets. Hydrodynamic modeling can be used to provide information that would be prohibitively expensive or impractical to observe synoptically in the field, and to hindcast historical conditions during the surveys to provide additional information that was not collected during the original surveys. Such information derived from hydrodynamic models can be used to improve the understanding of, or the ability to convey, the information in fisheries surveys data sets themselves. However, there are currently only a few examples of studies that have linked long-term biological sampling with state-of-the-art hydrodynamic modeling (e.g., Song et al. 2012; Bever et al. 2016).

This study had two primary objectives. The first objective was to validate a coarse-grid version of a three-dimensional (3-D) model of the estuary. The second objective was to combine recent advancements in hydrodynamic modeling capabilities with long-term fish monitoring data to improve communication among science, policy, and public audiences about the relationships between salinity and the abundance and distribution of native and resident fish populations. The ultimate goal of these efforts is to increase our understanding of the mechanistic relationships between salinity and fish abundance and to provide technical support for creating or modifying estuarine state water quality standards to protect aquatic life in the estuary. The EPA identified strengthening estuarine water quality standards as the most critical action under the Clean Water Act (CWA) to restore protection to beneficial uses for aquatic life in the 2012 San Francisco Bay Delta Action Plan (EPA 2012a).

Substantial advancements in Geographic Information System (GIS) mapping and hydrodynamic modeling have occurred since the mid-1990s when estuarine water quality standards were first adopted for the estuary. This study incorporates technological advancements by creating a GIS framework that imports salinity distribution maps developed using a 3-D hydrodynamic model and long-term fish monitoring data to produce a sequence of maps for six fishes. The sequence of maps visually illustrates the established connections between salinity and fish abundance statistically determined in prior studies (e.g., Jassby et al. 1995; Kimmerer 2002; Kimmerer et al. 2009) and, by adding the spatial information, expands both the understanding of, and the ability to convey, the relationships among salinity and fish abundance, distribution, and population resiliency.

The UnTRIM hydrodynamic model (Casulli and Zanolli 2002, 2005) has been implemented previously in the San Francisco Bay and Sacramento–San Joaquin Delta (MacWilliams et al. 2007, 2008, 2009, 2015). This "high-resolution" UnTRIM Bay–Delta Model, which MacWilliams et al. (2015) describe in detail, has been used previously to improve our understanding of the relationship between flow and the location of the 2 psu isohaline in the estuary (MacWilliams et al. 2015), to predict the effects on salinity of deepening navigation channels (MacWilliams et al. 2014), to investigate residence time in Clifton Court Forebay (MacWilliams and Gross 2013) and to investigate wave- and current-driven sediment transport within the estuary (Bever and MacWilliams 2013). However, it is very computationally intensive to predict the salinity distribution throughout large estuaries on decadal time-scales using high-resolution models.

As a result of recent advances in the numerical methods used in the UnTRIM model (Casulli 2009), it is possible to apply bathymetric data in UnTRIM at a resolution finer than the model grid on which hydrodynamic variables are calculated. This allows for the use of a coarser-resolution model grid, while still maintaining the ability to specify channel bathymetry in enough detail to preserve the cross-sectional area and volume of small channels (e.g., Sehili et al. 2014; Casulli and Stelling 2010). This approach was applied to San Francisco Bay to develop a "coarse-grid" version of the UnTRIM Bay–Delta model that was suitable for simulating long time periods. This model was applied to simulate a 35-year period between January 1, 1980 and December 31, 2014 and to develop salinity distribution maps that were suitable for visualizing fish density and distribution together on maps of salinity averaged over time periods relevant for each species. In addition, these simulations were used to evaluate the relationships between long-term trends in Delta outflow, X2, and the area and position of the Low Salinity Zone (LSZ).

METHODS

UnTRIM Bay–Delta Model

UnTRIM is a 3-D hydrodynamic model that solves the Navier–Stokes equations—which describe the motions of viscous fluids—on an unstructured horizontal grid and a z-level vertical grid. The numerical method allows full wetting and drying of each grid cell. The governing equations are discretized using a finite difference–finite volume algorithm. The governing equations, numerical discretization, and numerical properties of UnTRIM are described in Casulli and Zanolli (2002, 2005), Casulli (1999, 2009), and Casulli and Walters (2000) and are not reproduced here.

The high-resolution UnTRIM San Francisco Bay–Delta model (UnTRIM Bay–Delta model) is a 3-D hydrodynamic model of San Francisco Bay and the Sacramento–San Joaquin Delta (Delta), which has been developed using the UnTRIM hydrodynamic model (MacWilliams et al. 2007, 2008, 2009, 2015). The high-resolution UnTRIM Bay–Delta model extends from approximately the Gulf of the Farallones in the Pacific Ocean through the entire Bay–Delta and takes advantage of the grid flexibility allowed in an unstructured mesh by gradually varying grid cell sizes, beginning with large grid cells in the Pacific Ocean and gradually transitioning to finer grid resolution in the smaller channels of the Sacramento–San Joaquin Delta. This approach offers significant advantages in both numerical efficiency and accuracy, and allows for local grid refinement for detailed analysis of local hydrodynamics, while the overall hydrodynamics of the entire estuary are still incorporated in a single model. The resulting high-resolution model contains more than 130,000 horizontal grid cells and more than 1 million 3-D grid cells.

The high-resolution UnTRIM Bay–Delta model simulations typically run slightly faster than 30 times real-time on a desktop workstation, which allows 1 calendar year to be simulated in approximately 12 days. Thus, using the high-resolution model, the simulation of a 35-year period would require more than a year of simulation time. To allow for longer simulations, a model of San Francisco Bay and the Sacramento–San Joaquin Delta has also been developed on a coarse-resolution grid using UnTRIM. The coarse-grid Bay–Delta model makes use of an unstructured grid, similar to that of the high-resolution model, but also incorporates the bathymetry on the grid at a resolution higher than the hydrodynamic model grid itself, as described in Casulli (2009). Thus, within each grid cell and along each grid edge, the bathymetry can be specified at a resolution higher than the resolution at which the hydrodynamic model calculations are made (Figure 1).

"Subgrid" bathymetry allows for the specification of nearly identical bathymetry on the coarse-grid UnTRIM Bay–Delta model, but uses significantly fewer hydrodynamic grid cells than in the high-resolution model, which greatly reduces model run times. For example, in the region surrounding Mildred Island in the Delta, the high-resolution UnTRIM Bay–Delta model uses 6,508 2-D cells in the region shown (Figure 2A), whereas the coarse-grid UnTRIM Bay–Delta model grid uses 329 2-D cells (Figure 2B). The model domain and boundary conditions of the coarse-grid model (Figure 3) are nearly identical to the high-resolution model (see Figure 2 in MacWilliams et al. 2015). Both models have identical vertical resolution and use a total of

http://dx.doi.org/10.15447/sfews.2016v14iss2art3

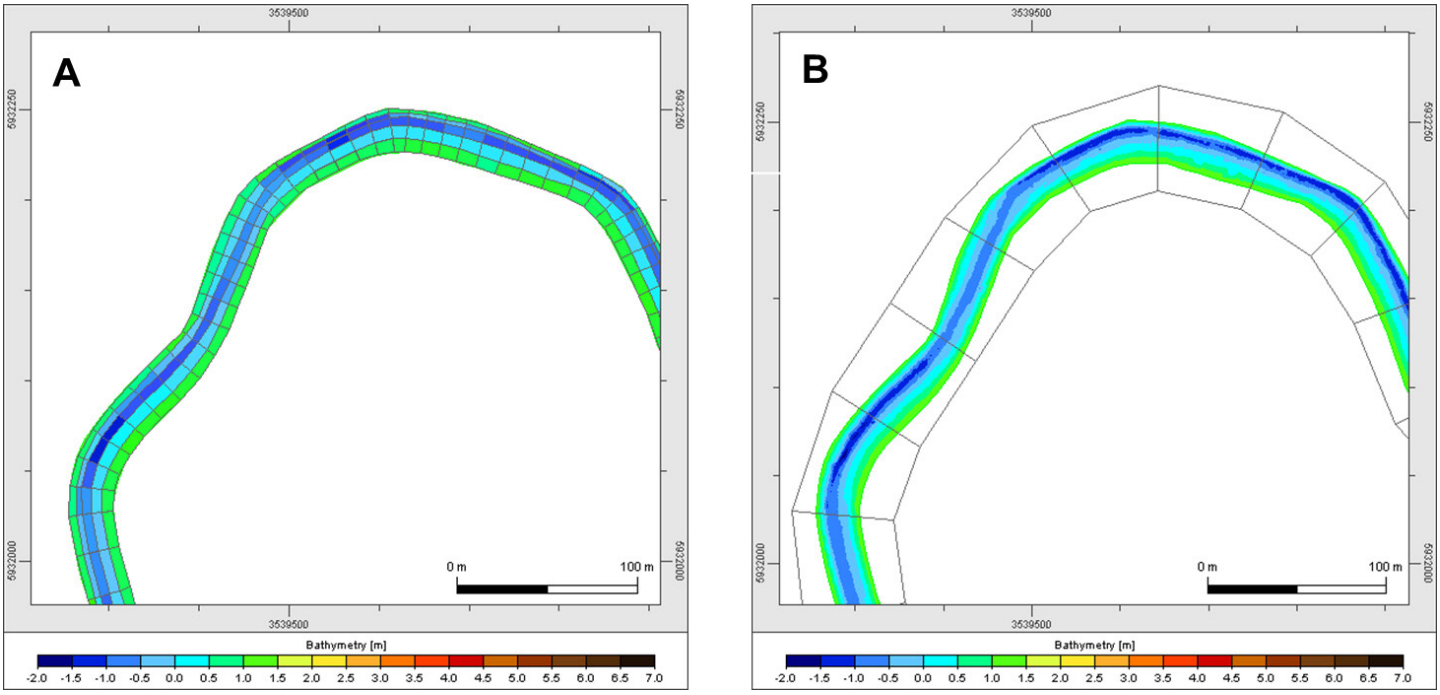

Figure 1 (A) Classic UnTRIM grid used in high-resolution model with five cells across channel to resolve channel bathymetry; **(B)** UnTRIM grid with subgrid bathymetry used in coarse resolution model with one cell across channel to resolve channel bathymetry at a subgrid scale. Source: Lippert (2009).

47 vertical layers. A 1-m vertical resolution is used to a depth of 20 m below zero NAVD88 and the vertical layer spacing gradually increases from 1 m to 5 m between 20 m below zero NAVD88 and 105 m below zero NAVD88. However, the coarse-grid UnTRIM Bay–Delta model can run faster than 1,200 times real time on a desktop workstation, which allows 1 calendar year to be simulated in approximately 7.5 hours, and the 35-year period that is part of this study to be simulated in approximately 10.5 days.

The high-resolution UnTRIM Bay–Delta model has been calibrated using water level, flow, and salinity data collected in San Francisco Bay and the Delta in numerous previous studies (e.g., MacWilliams et al. 2008, 2009, 2015). The model has been shown to accurately predict salinity, tidal flows, and water levels throughout the San Francisco Bay and Sacramento–San Joaquin Delta under a wide range of conditions. To date, the calibration of the coarse-grid UnTRIM Bay–Delta model has not been extensively documented. This paper summarizes the detailed model validation conducted for the coarse-grid UnTRIM Bay–Delta model, and assesses how well the coarse-grid UnTRIM Bay–Delta model predicts the salinity field in the estuary. We also compare the predictions of X2 and the LSZ area from the coarse-grid model to the predictions from the high-resolution model, to demonstrate that the long-term time-series predictions were suitable to investigate changes in X2 and the LSZ area over decadal time-periods.

Model Validation for 1994–1997 Period

MacWilliams et al. (2015) presented a detailed validation of the high-resolution UnTRIM Bay–Delta model using all available data over a 3-year period that spanned from April 1, 1994 through April 1, 1997. This 3-year model simulation period spans parts of 4 water years, which encompassed a large part of the historical range of Delta outflows. Water years 1994 (October 1, 1993 through September 30, 1994) through 1997 ranked 6th, 54th, 40th, and 48th, respectively, in annual mean Delta outflow over the 57-year record (CDWR 2013). January 1997 had the second-highest monthly mean outflow, and

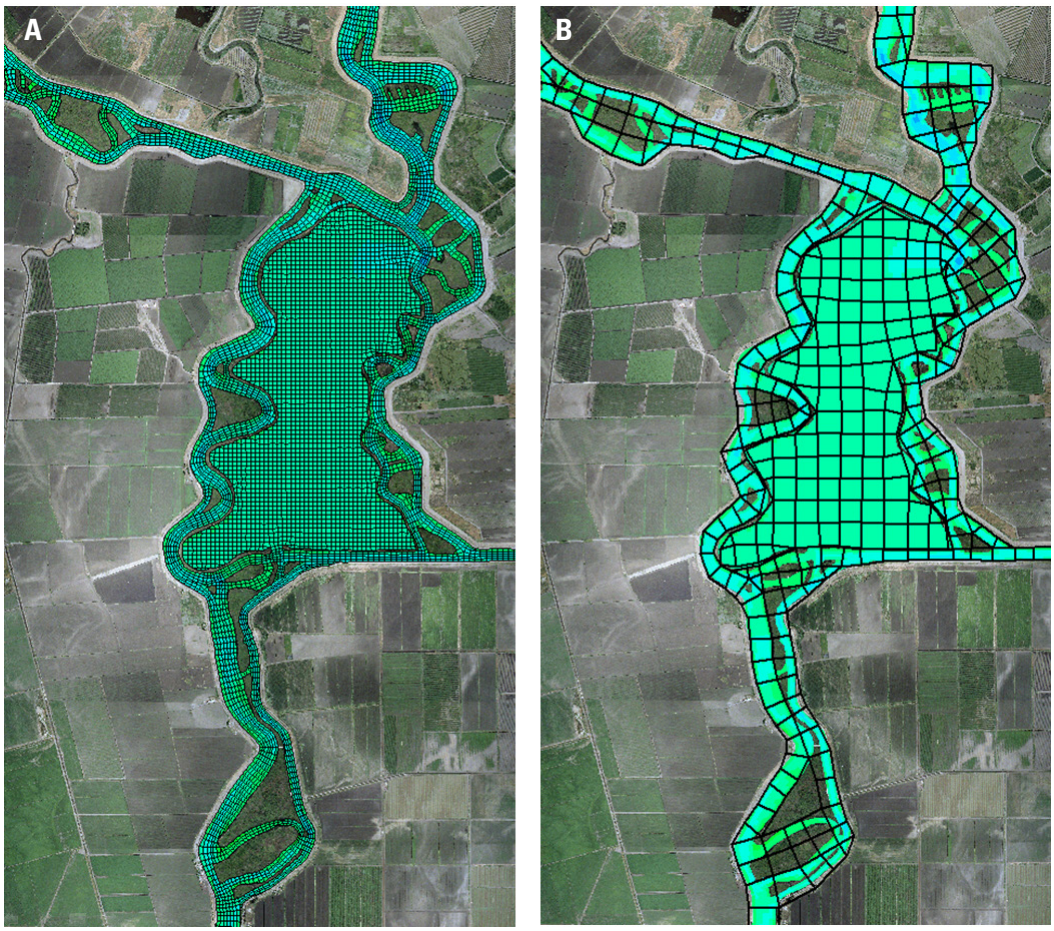

Figure 2 Comparison of model grids in the region of Mildred Island from **(A)** the high-resolution UnTRIM Bay–Delta model grid; **(B)** the coarse-resolution UnTRIM Bay–Delta model grid

January 1, 1997 the second-highest daily outflow, in the record. MacWilliams et al. (2015) also presented a detailed approach for evaluating model accuracy and the quality of fit between the observation data and model predictions of water level, tidal flows, and salinity that entails the use of both model skill (Willmott 1981) and target diagrams (Jolliff et al. 2009; Hofmann et al. 2011). Both the model skill and target diagram statistics provide quantitative metrics for the agreement of the model predictions with the observations. The target diagrams also visually demonstrate the relationship between the means and the variances of the predictions and observations. Target diagrams show the bias in the predictions normalized by the observed standard deviation ($bias_N$) on the y-axis and the unbiased root-mean-square difference normalized by the observed standard deviation ($ubRMSD_N$) on the x-axis. Points which plot on the positive y-axis show the model over predicts the mean of the observations, while points which plot on the positive x-axis show the model over predicts the variability in the observations. More details on target diagrams and their use in model skill assessment can be found in Jolliff et al. (2009). Using the quantitative accuracy evaluation thresholds shown in Table 1, we used both model skill and target diagrams to evaluate the accuracy of the coarse-grid Bay–Delta model for predicting water level, tidal flows and salinity over the same 3-year period. Detailed comparisons between observed and predicted time series were made at 34 locations for water levels, 6 locations for flows, and 38 locations for salinity.

http://dx.doi.org/10.15447/sfews.2016v14iss2art3

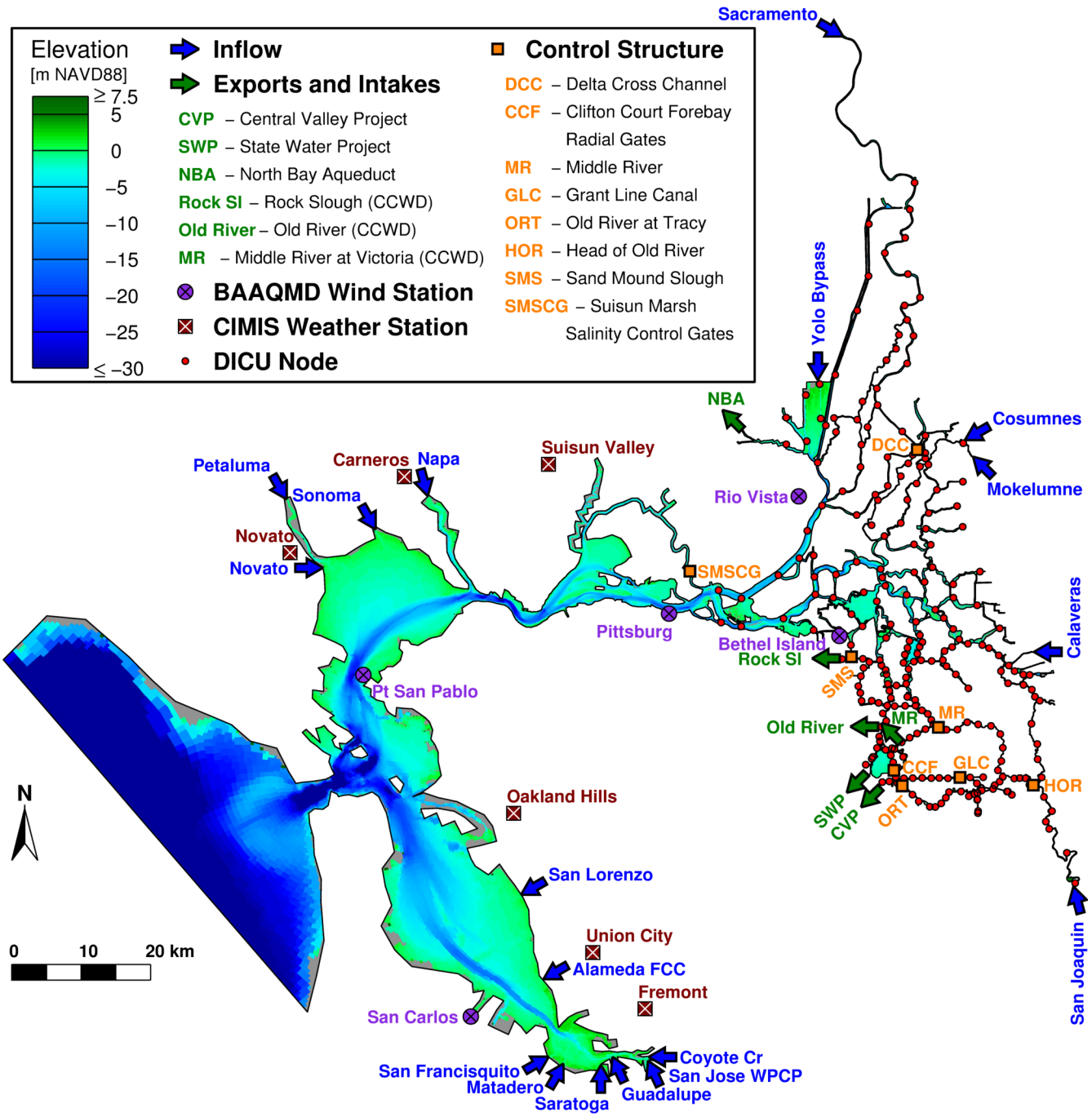

Figure 3 Model domain, bathymetry, and locations of model boundary conditions which include inflows, Delta export facilities and Contra Costa Water District (CCWD) intakes, wind stations from the Bay Area Air Quality Management District (BAAQMD), evaporation and precipitation from the California Irrigation Management System (CIMIS) weather stations, Delta Island Consumptive Use (DICU), and flow control structures

Model Validation using Salinity Observations from Fish Sampling Data (1980–2012)

We developed a method that incorporated data from three long-term fisheries surveys to validate the spatial distribution of salinity throughout the estuary. Since the 1960s boat-based fisheries surveys have been conducted regularly throughout the San Francisco Bay and Sacramento–San Joaquin Delta (Turner and Chadwick 1972; Stevens and Miller 1983; Armor and Herrgesell 1985; CDFW 2015). Along with fish catch data, the fisheries surveys also recorded environmental variables at each of the stations sampled. For example, most of the surveys measured surface conductance (which can be mathematically converted to salinity), water temperature, and Secchi depth. We compared the predicted surface salinity from the coarse-grid simulations to the surface salinity observed by the fisheries surveys to validate the model predictions of the spatial salinity distribution from San Pablo Bay through the Delta. We compared observed and predicted surface salinity when and where surface salinity observations were made as part of either the Fall Midwater Trawl (FMWT) Survey, the Summer Townet Survey, or the San Francisco Bay Study (Bay Study) fish data collection cruises during the 35-year simulation period (Figure 4). The fisheries survey data were not available for 2013 or 2014 when we conducted this analysis, so we validated predicted surface salinity from 1980 through 2012. The validation of predicted surface salinity was conducted by using target diagram statistics and scatter plots to validate each simulated year separately.

X2 and LSZ Validation

For each day during the 35-year simulation period, we calculated X2 as the distance from the Golden Gate to the location where the predicted daily-averaged near-bed salinity was 2 psu (Jassby et al. 1995). We used the daily-averaged near-bed salinity along two transects following the axis of the estuary from the Golden Gate to the Sacramento–San Joaquin Delta to calculate X2 (see Figure 3 in MacWilliams et al. 2015). For X2 > 75 km, we calculated X2 as the average of the distance along the Sacramento River and San Joaquin River transects.

For each day during the simulation period, we calculated the predicted spatial extent of the LSZ and related it to the predicted X2. For this analysis, we defined the LSZ as the region where the depth-averaged salinity was between 0.5 and 6.0 psu. To compute the area of the LSZ for each day, we then summed the area of the wet portion of the subgrid with daily-averaged depth-averaged salinity between 0.5 and 6.0 psu within each hydrodynamic grid cell from San Pablo Bay into the Delta (Figure 3).

We extracted the predicted time-series of X2 and the area of the LSZ calculated from the coarse-grid UnTRIM Bay–Delta model from April 1, 1994 to April 1, 1997 from the 35-year simulation, and compared them to the previously published predictions of X2 and LSZ area from the high-resolution model (MacWilliams et al. 2015). Because the salinity predictions from the high-resolution model have been extensively validated both spatially and temporally in numerous previous studies (e.g., MacWilliams et al. 2007, 2008, 2009, 2015), comparing the X2 and LSZ predictions from the high-resolution and coarse-

Table 1 Thresholds for evaluating model accuracy based on model skill (Willmott 1981) and the radii of circles on the target diagram (Jolliff et al. 2009) established by MacWilliams et al. (2015)

Model accuracy		Water level	Flow	Salinity	Current speed
Skill accuracy	Accurate	>0.975	>0.975	>0.85	>0.9
	Acceptable	0.95 - 0.975	0.95 - 0.975	0.7-0.85	0.8-0.9
	Poor Agreement	<0.95	<0.95	<0.7	<0.8
Target accuracy	Very Accurate	0.0 - 0.25			
	Accurate	0.25 - 0.5			
	Acceptable	0.5 - 1.0			
	Poor Agreement	> 1.0			

http://dx.doi.org/10.15447/sfews.2016v14iss2art3

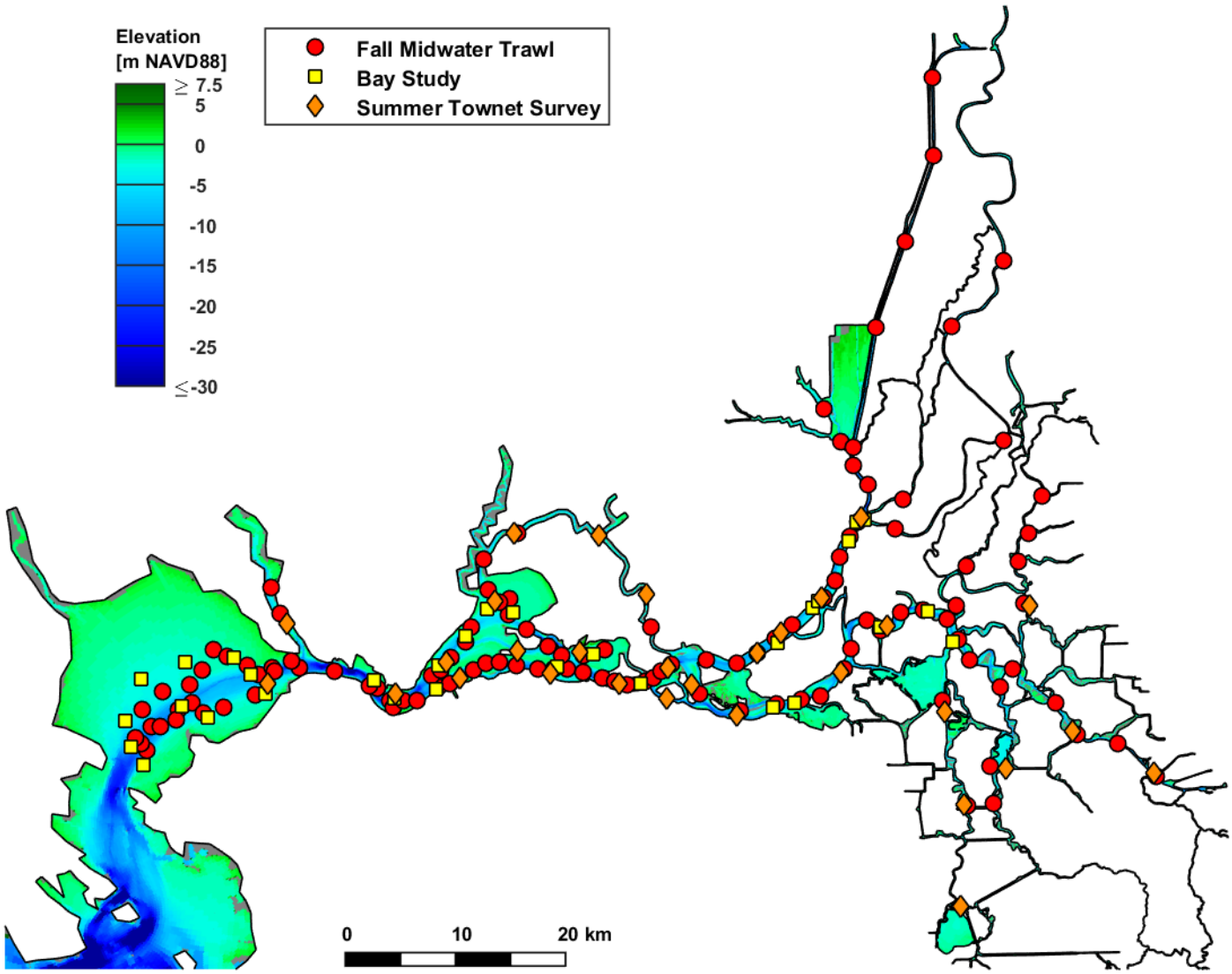

Figure 4 Location of subset of Fall Midwater Trawl stations, San Francisco Bay Study stations, and Summer Townet Survey stations used in the validation of the surface salinity

grid models provides a method to assess whether the position of X2 and the area of the LSZ are adequately represented on the coarse grid.

Long-Term Trends in Salinity Distribution and LSZ Area

Previous analyses of trends in LSZ area (e.g., MacWilliams et al. 2015) have been limited to the duration of simulations that were computationally feasible using the high-resolution model. We used the predicted X2 and LSZ area for each day between January 1, 1980 and December 31, 2014 to explore seasonal and annual differences in both X2 and LSZ area over the 35 years simulated using the coarse-grid model. This analysis focused on long-term trends in Delta outflow, X2, and LSZ area during the fall period between September 1 and November 30 of each year simulated. To investigate possible long-term changes in the LSZ area, we also evaluated the percent of days between September 1 and November 30 during each year that the LSZ area was predicted to be greater than 75 km^2. We performed Spearman's rho and Kendall's tau rank correlations to test for a

significant trend in the September through November average Delta outflow, X2, LSZ area, and on the percent of the days that the LSZ was greater than 75 km^2. A ranked correlation is appropriate because there is no reason to assume any trends will be linear.

Salinity Field and Fish Abundance and Distribution

We used GIS (ArcMap 10.2.1) to combine 33 years (1980–2012) of salinity predictions with fish abundance data collected by the San Francisco Bay Study (Armor and Herrgesell 1985; Baxter et al. 1999). We combined salinity distributions predicted using the coarse-grid UnTRIM Bay–Delta model with catch per unit effort (CPUE) data for six fishes (EPA 2015): Delta Smelt (*Hypomesus transpacificus*), Longfin Smelt (*Spirinchus thaleichthys*), Pacific Herring (*Clupea pallasi*), Sacramento Splittail (*Pogonichthys macrolepidotus*), Starry Flounder (*Platyichthys stellatus*), and Striped Bass (*Morone saxatilis*). For each fish listed, we calculated the annual average CPUE at each monitoring station for each of the 33 years. For each year during the analysis period, we calculated a total of seven salinity distribution maps from the predictions of daily-averaged depth-averaged salinity for species-specific averaging periods correlated with the annual CPUE of each fish species (Table 2). We chose species-specific periods for averaging and the corresponding fishes age-classes based on Kimmerer (2002), with the salinity averaging periods selected to roughly correspond to larval and juvenile life stages of the subject fishes. We selected salinity averaging periods based on juvenile life stages because survival in early life stages is generally considered essential for producing strong year classes when density dependence is not evident. However, age–0 Longfin Smelt were plotted on a shorter salinity averaging period (May – June) than identified by Kimmerer (2002) to isolate the months that juveniles are large enough to be caught by trawl nets. One example which compares two different maps for age–0 Longfin Smelt is presented below. The complete set of 231 salinity distribution and CPUE maps is available from EPA (2015).

RESULTS

Model Validation for 1994–1997

Using the same model skill and target diagram accuracy criteria used by MacWilliams et al. (2015), the comparison of the quality of fit between the observation data and model predictions indicates that the coarse-grid model predicts water level (34 locations), tidal flow (6 locations), and salinity (38 locations) with a level of accuracy similar to the high-resolution model (Table 3). A representative time-series comparison (Figure 5) between the observed and predicted salinity at the surface sensor at the Sacramento River near Mallard Island station, where the salinity is typically within the range of the LSZ (analogous to Figure 10 in MacWilliams et al. 2015), shows the model accurately predicts the timing and magnitude of tidal and seasonal variability in the salinity. Based on the skill accuracy criteria (Table 1), the same number of stations are classified as accurate and acceptable for salinity predictions from the coarse-grid model as from the high-resolution model; at the flow and water level stations the high-resolution model performs slightly better based on the skill metric. A comparison of the target diagrams shows that the quality of fit between the observation

Table 2 Fish species and seasonal averaging periods used to develop fish and salinity distribution maps

Species maps	Abundance data	Salinity averaging period	Age class
Delta Smelt	Annual mean CPUE	February – June	All ages
Longfin Smelt (juvenille)	Annual mean CPUE	May – June	Age 0
Longfin Smelt	Annual mean CPUE	January – June	All ages
Pacific Herring	Annual mean CPUE	January – April	Age 1
Sacramento Splittail	Annual mean CPUE	February – May	All ages
Starry Flounder	Annual mean CPUE	March – June	Age 1
Striped Bass	Annual mean CPUE	April – June	Age 0

http://dx.doi.org/10.15447/sfews.2016v14iss2art3

Table 3 Summary of the number and percent of stations classified as very accurate, accurate, acceptable, and poor accuracy based on the model skill and the target diagram accuracy thresholds shown in Table 1 for the 1994–1997 simulation period from the high-resolution UnTRIM Bay–Delta model and from the coarse-grid UnTRIM Bay–Delta model used in this study.

		High-resolution UnTRIM Bay–Delta Model 1994–1997 [a]			Coarse-grid UnTRIM Bay–Delta Model 1994–1997 [b]		
		Water level	Flow	Salinity	Water level	Flow	Salinity
Skill accuracy	Accurate	30 (88%)	5 (83%)	29 (76%)	27 (80%)	4 (67%)	29 (76%)
	Acceptable	3 (9%)	1 (17%)	4 (11%)	5 (14%)	2 (33%)	4 (11%)
	Poor accuracy	1 (3%)	0	5 (13%)	2 (6%)	0	5 (13%)
Target accuracy	Very accurate	23 (67%)	4 (67%)	5 (13%)	21 (62%)	4 (67%)	1 (3%)
	Accurate	10 (30%)	2 (33%)	18 (48%)	12 (35%)	2 (33%)	24 (63%)
	Acceptable	1 (3%)	0	9 (24%)	1 (3%)	0	7 (18%)
	Poor accuracy	0	0	6 (15%)	0	0	6 (16%)

a. Source: MacWilliams et al. 2015.
b. Source: this study.

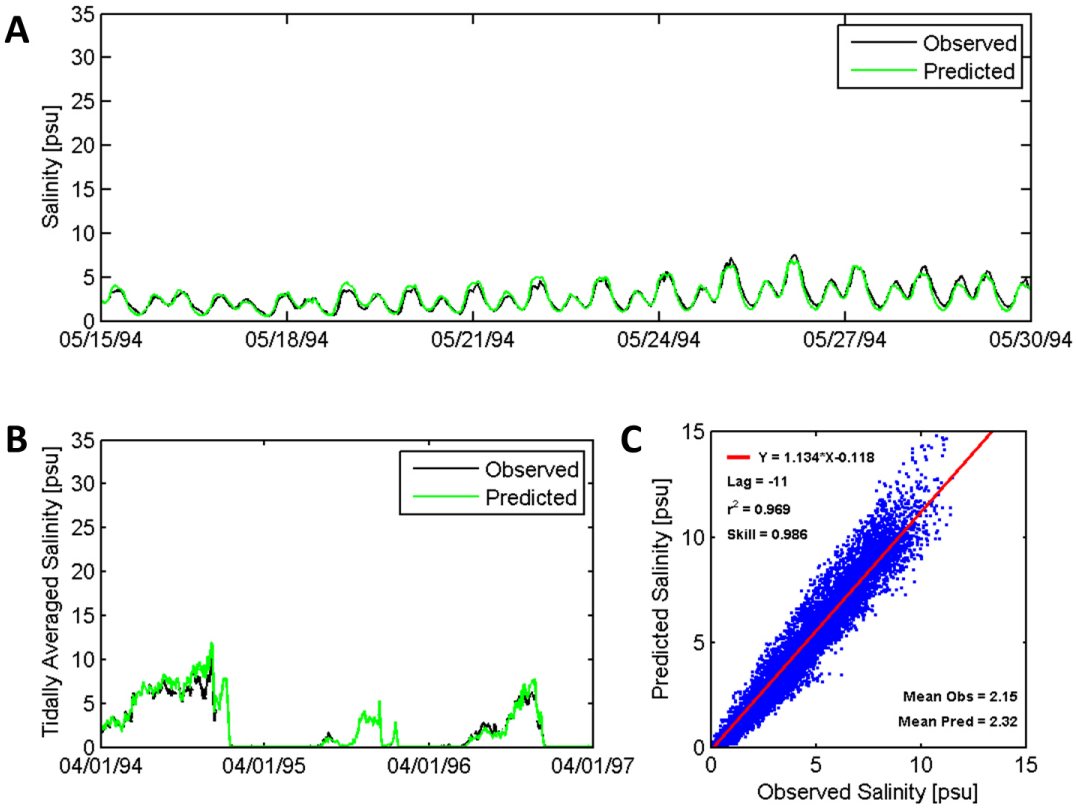

Figure 5 Observed and predicted salinity from the surface sensor at the Sacramento River near Mallard Island station during the 1994–1997 simulation period

data and model predictions of water level, tidal flows, and salinity for the coarse-grid model (Figures 6A through 6C) and for the application of the high-resolution model (Figures 6D through 6F) over the same period demonstrates the accuracy of the coarse-grid model is very similar to the accuracy of the high-resolution model. Based on the target accuracy criteria, the coarse-grid model salinity predictions yield four fewer stations classified as very accurate than the high-resolution model, but two fewer stations classified as acceptable (Table 3). Overall, this results in a net increase in the total number of stations where salinity predictions were classified as either accurate or very accurate.

Model Validation Using Salinity Observations from Fish Sampling Data (1980–2012)

The model accurately (inside radius 0.5) to very accurately (inside radius of 0.25) predicted the spatial distribution of the surface salinity measurements for each of the 33 years between 1980 and 2012 (Figure 7). The model tended to predict slightly higher salinity in the late 1980s than was observed (as indicated by 85, 87, and 88 appearing highest on the *y*-axis of the target diagram). However, even in years when the model predicted higher surface salinity than was observed, it still captured the gradient in the surface salinity from San Pablo Bay through the Delta (Figure 8). Figure 8A highlights that even in 1988 when the predicted salinity tended to be higher than the observed salinity, the slope of the best-fit line comparing the observed to predicted salinity

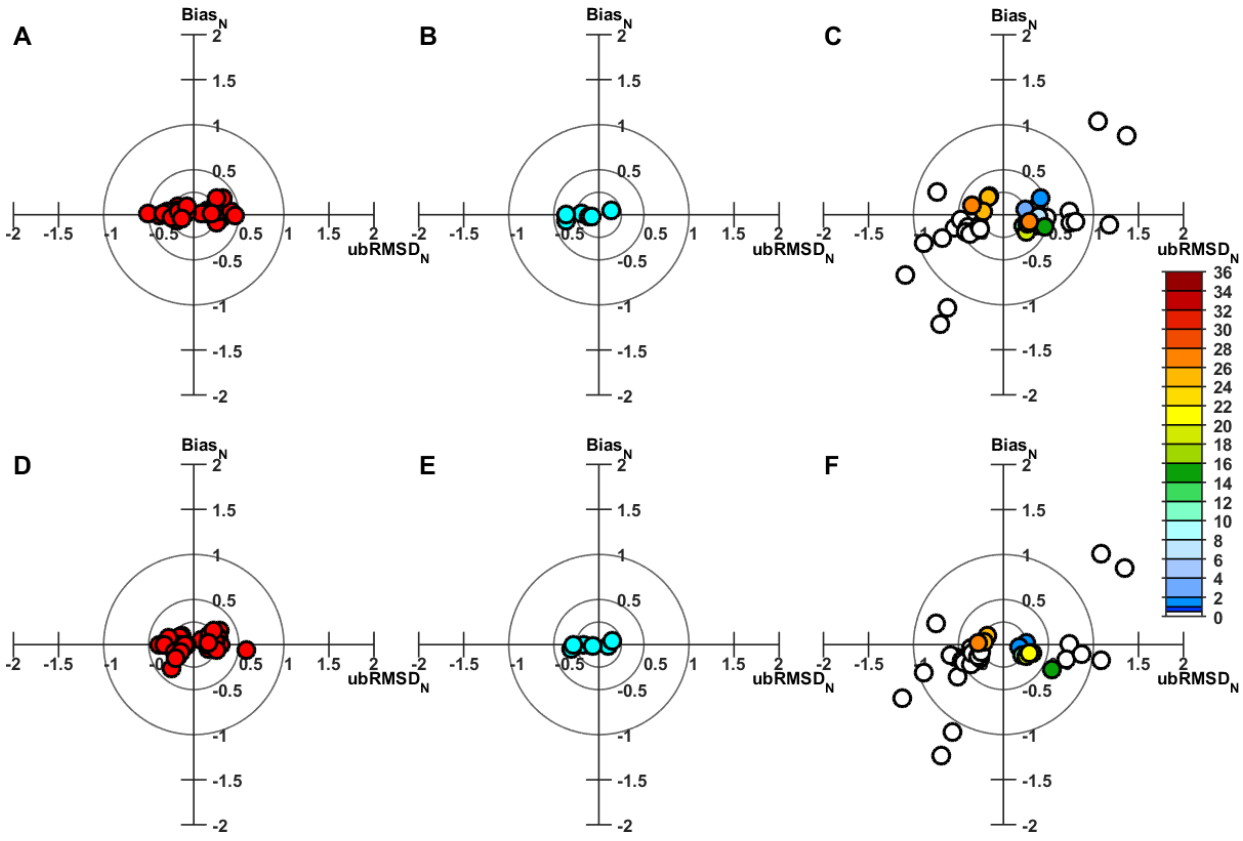

Figure 6 Target diagrams summarizing how the model predictions from the coarse-grid UnTRIM Bay–Delta model compare to the observed time-series data during 1994–1997 for **(A)** water level, **(B)** tidal flow, and **(C)** salinity; and how the predictions from the high-resolution UnTRIM Bay–Delta model presented in MacWilliams et al. (2015) compare to the same observed time-series for **(D)** water level, **(E)** tidal flow, and **(F)** salinity. Symbols for salinity are colored based on the average predicted salinity at each station for both the high-resolution and coarse-grid models.

http://dx.doi.org/10.15447/sfews.2016v14iss2art3

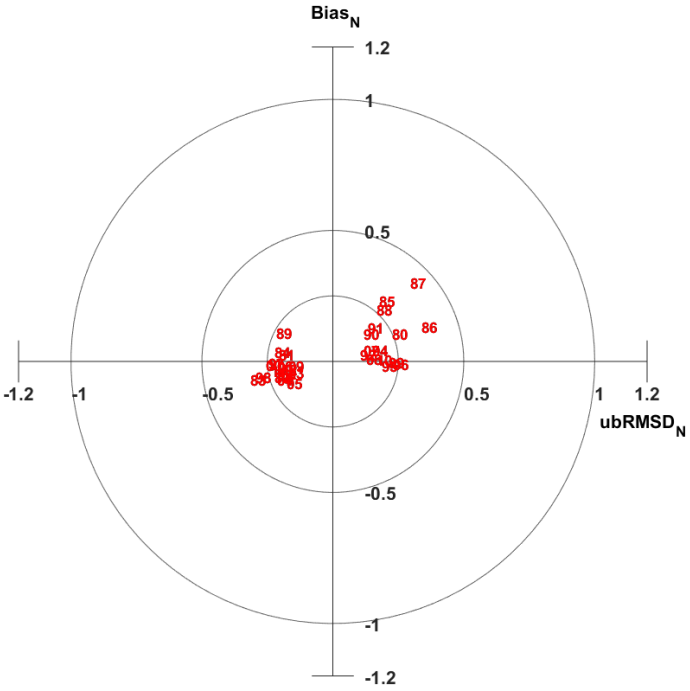

Figure 7 Target diagram showing the yearly model validation of the spatial distribution of the surface salinity measured by the fish monitoring programs

was near one (0.999) and the r^2 value was still high (0.963), indicating the model predicted a very similar decrease in salinity from west to east as was seen in the survey observations of surface salinity. In years when the model predicted the salinity most accurately, such as 2008, the best-fit line between the observed and predicted surface salinity overlaid the 1:1 line, indicating the model nearly exactly captured the estuary-wide salinity gradient from the observations (Figure 8B).

X2 and LSZ Validation

The coarse-grid UnTRIM Bay–Delta model predicts very similar values of both X2 and the LSZ area to those the high-resolution model predicts (Figure 9). The predictions of X2 show very little scatter around the 1:1 line (Figure 10A), while the predictions of LSZ area show slightly more scatter (Figure 10B) but still have a high r^2 value (0.951).

Long-Term Trends in Salinity Distribution and LSZ Area

The 35-year time-series of Delta outflow, predicted X2, and predicted LSZ area highlight the large amount of seasonal and interannual variability (Figure 11). The influence of short-duration weather patterns on the salinity distribution in the estuary is highlighted by the abrupt increase and then decrease in the LSZ area. Episodic winter storms quickly increase the freshwater flow into the estuary (Figure 11A), resulting in a sharp decrease in X2 (Figure 11B), and a corresponding increase in the area of the LSZ (Figure 11C). The recurring seasonal pattern of increasing LSZ area in the winter followed by a more gradual decrease throughout the year is evident in the 35-year time-series of the LSZ area (Figure 11C).

In order to highlight the fall periods, the values of outflow, X2 and LSZ area between September 1 and November 30 of each year are highlighted in black on Figure 11. December was not included in the fall period because the salinity distribution during December is strongly influenced by whether the first flush occurs before, during, or after December. Low values of the LSZ area (LSZ area $<75\,km^2$ indicated by yellow shading on Figure 11) occur both when X2 is between about 45 and 65 km and when X2 is between 75 and 95 km, which correspond to local minimums in the LSZ area (see Figure 12 in MacWilliams et al. 2015).

To evaluate long-term trends in Delta conditions during fall, we calculated average Delta outflow, average X2, average LSZ area, and the percentage of time that the LSZ area was greater than 75 km^2 during the 3-month period between September 1 and November 30 for each year during the simulation (Figure 12). The model predictions show generally less variability in the average LSZ area between September and November after about 2000, with all 7 years with the lowest predicted average LSZ area between September and November occurring between 2000 and 2014 (Figure 12C). Between 1980 and 2000, there were only 2 years when the area of the LSZ was not predicted to be greater than 75 km^2 on any days during September through November. However, during 9 of the 15 years since 2000, the area of the LSZ was not predicted to be greater than $75\,km^2$

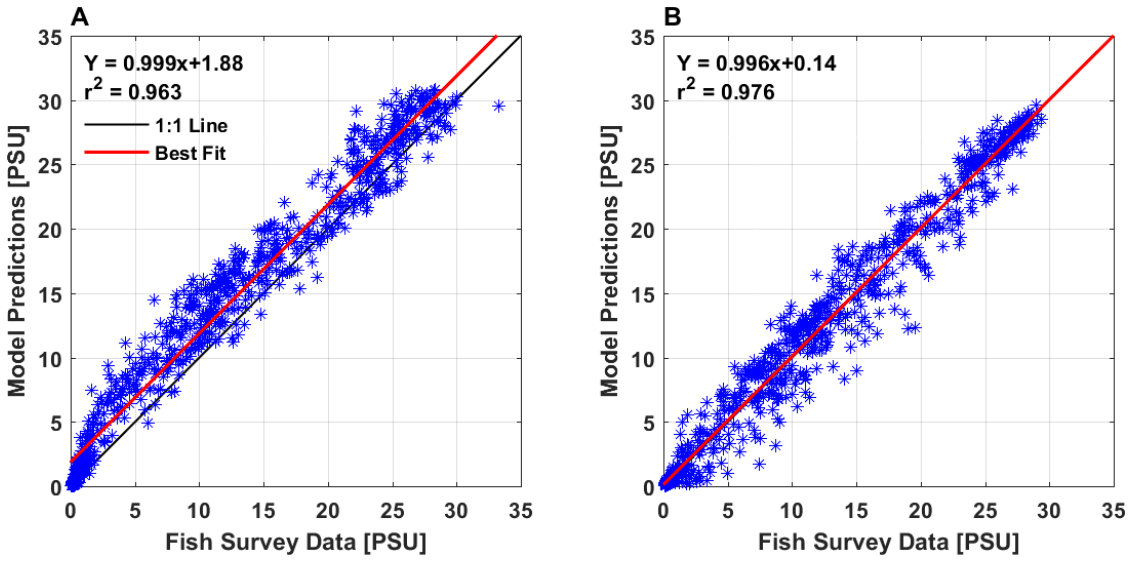

Figure 8 Scatter plots showing each observed and predicted data point in the surface salinity validation for **(A)** 1988 and **(B)** 2008. The equation of the best fit line and the coefficient of determination (r^2) are shown in the upper left of each panel.

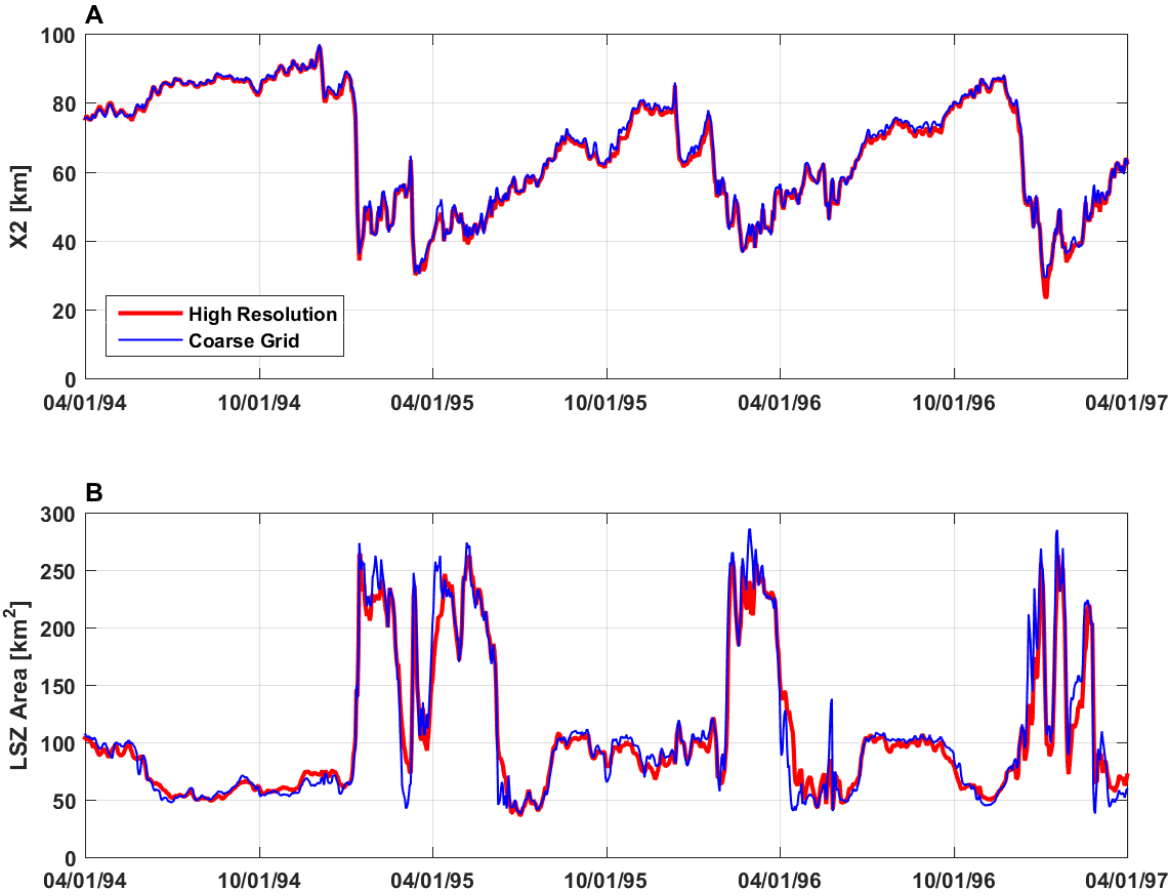

Figure 9 Comparison of predicted **(A)** X2 and **(B)** LSZ area for the high-resolution model (red) from MacWilliams et al. (2015) and the coarse-grid model (blue)

http://dx.doi.org/10.15447/sfews.2016v14iss2art3

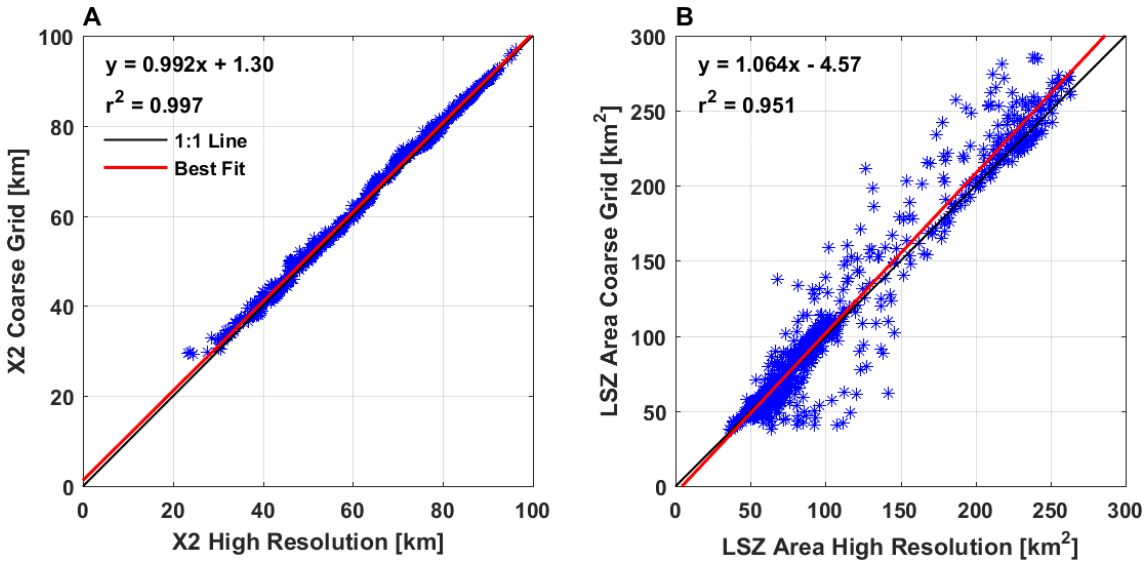

Figure 10 Comparison of predicted **(A)** X2 and **(B)** LSZ area from the high-resolution model from MacWilliams et al. (2015) and the coarse-grid model for each day during the 1994–1997 model simulation period

on any days during September through November (Figure 12D). Both the Spearman's rho and Kendall's tau rank correlations demonstrate a significant trend of decreasing fall average LSZ area from 1980 to 2014, and in the percentage of the time between September and November that the LSZ area is greater than 75 km^2 over this same time-period (Table 4). However, both tests indicate there has not been a significant trend in fall average Delta outflow from 1980 through 2014, and that there may be only a very weakly significant trend in increasing X2 from 1980 to 2014 between September and November (Table 4).

Salinity Field and Fish Abundance and Distribution

Visualization of the predicted average salinity distribution between May 1 and June 30 with the annual average CPUE of age–0 Longfin Smelt for each monitoring station in the San Francisco Bay Study midwater trawl during 1981 (Figure 13A) and 1982 (Figure 13B) shows that the fish density and distribution of age–0 Longfin Smelt was much larger during 1982 when salinity during May and June was lower in San Pablo and Suisun Bay.

DISCUSSION

Applicability of High-Resolution and Coarse-Grid Implementations of UnTRIM Bay–Delta Model

Because the model domain and boundary conditions of the coarse-grid UnTRIM Bay–Delta model (Figure 3) are nearly identical to the high-resolution model (see Figure 2 in MacWilliams et al. 2015), one or both model grids can be applied using the same boundary conditions and UnTRIM model code, depending on the needs of a specific application. The comparisons between the predictions of X2 and LSZ area from the high-resolution model and the coarse-grid model used in this study indicate that the coarse-grid model predicts extremely similar values of both X2 and LSZ area to those predicted using the high-resolution model (Figure 9 and 10). This may result, in part, because both models have the same vertical resolution and use the same turbulence model, and are therefore equally well-suited to simulate baroclinic forcing, which is one of the primary drivers of salt intrusion into the estuary.

The comparison of LSZ area between the coarse-grid and high-resolution models indicates more scatter than the predictions of X2 (Figure 10). The small amount of scatter in the X2 plot results, in part, from how X2 is calculated from the model salinity predictions. For both the high-resolution and

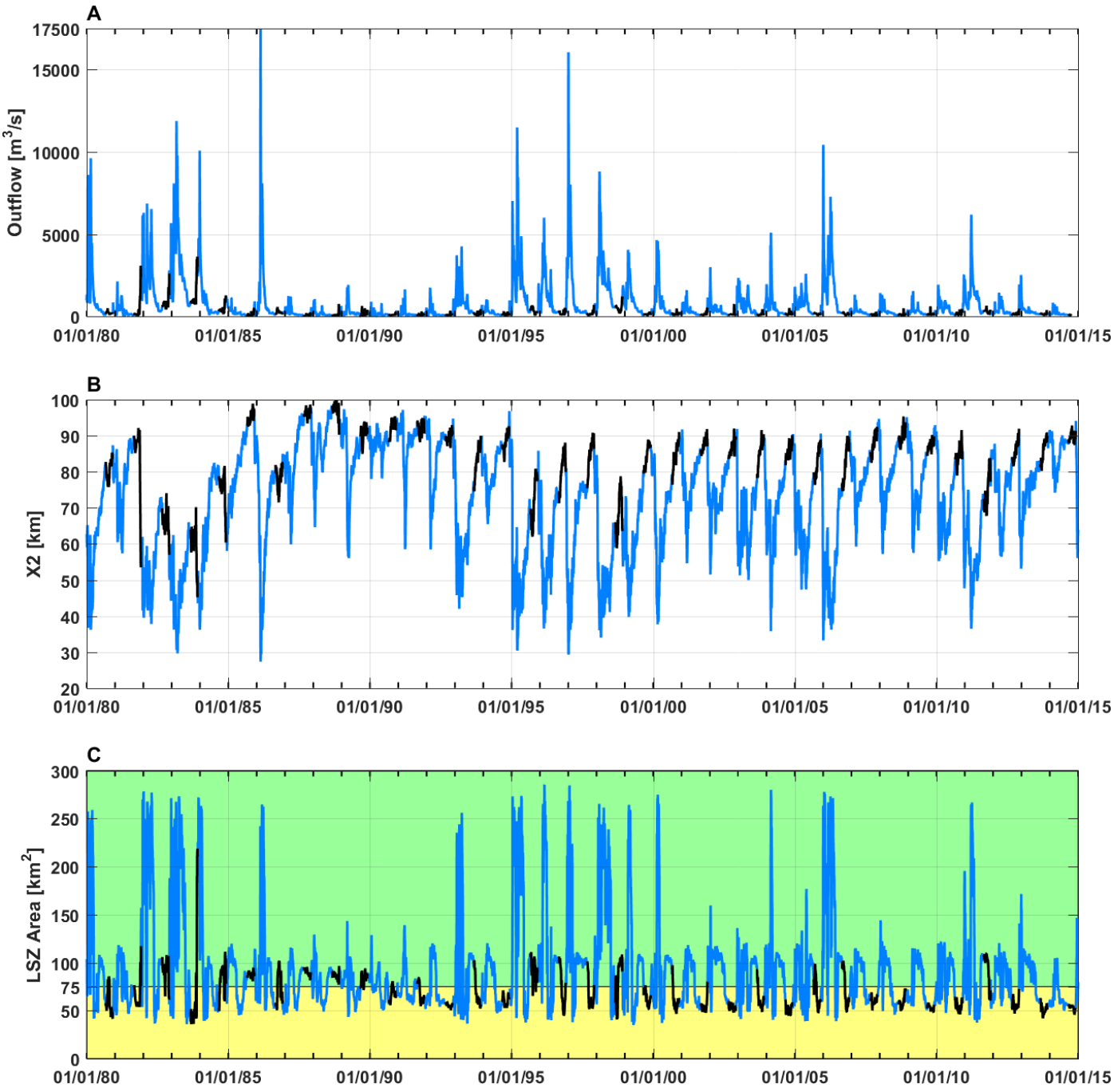

Figure 11 Predicted daily values of **(A)** outflow **(B)** X2 and **(C)** LSZ area from the coarse-grid model. Fall periods between September 1 and November 30 are highlighted in black.

http://dx.doi.org/10.15447/sfews.2016v14iss2art3

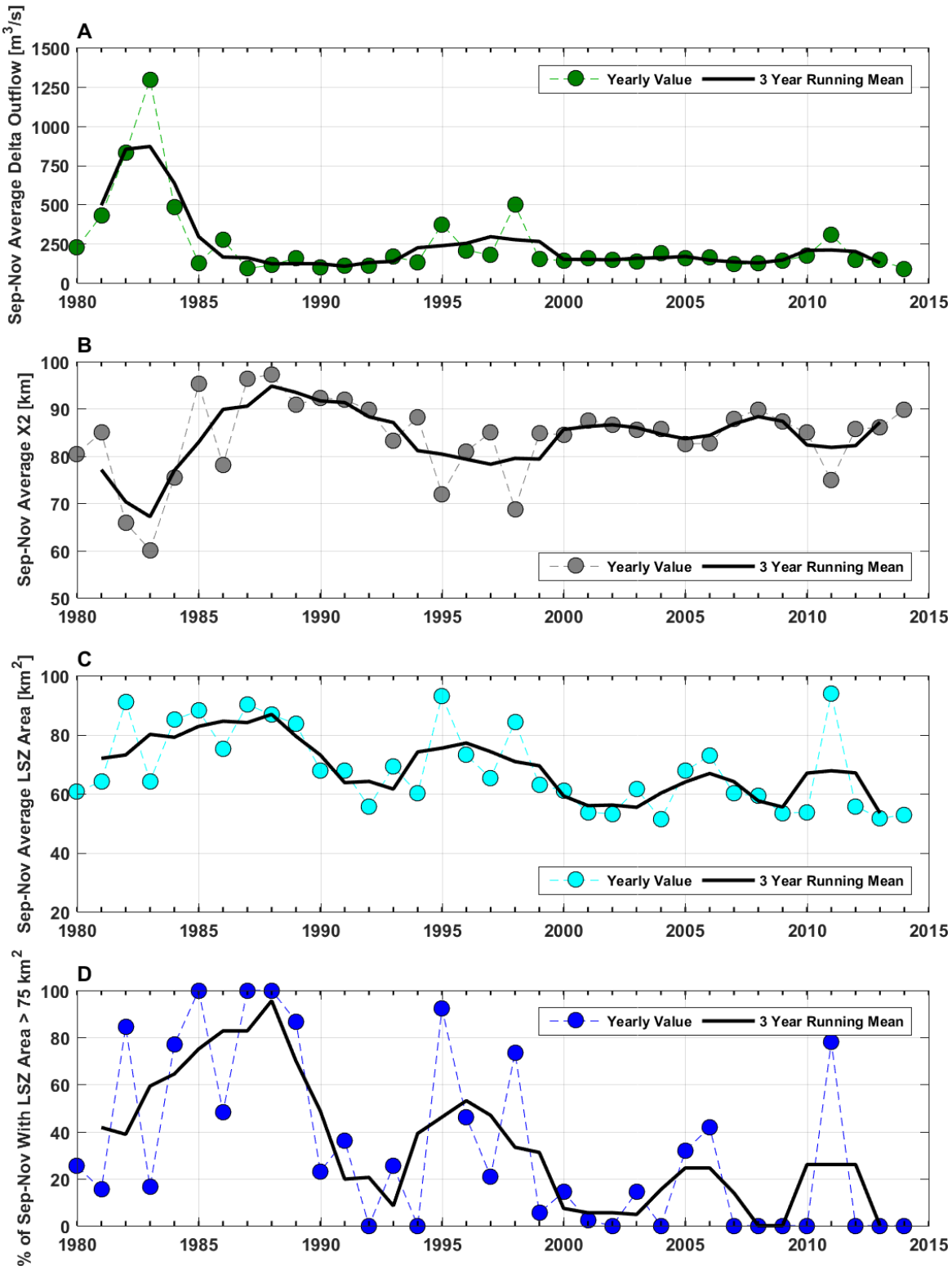

Figure 12 **(A)** Average outflow from September through November, **(B)**, Average X2 for September through November, **(C)** Average LSZ area for September through November, and **(D)** percent of days between September 1 and November 30 each year that the LSZ area was greater than 75 km^2

Table 4 Spearman's rho and Kendall's tau rank correlation tests on the September through November average Delta outflow, X2, LSZ area, and the percentage of days the LSZ area is greater than 75 km^2 for the period between 1980 through 2014

September – November	Spearman		Kendall	
	rho	*p*	*tau*	*p*
Average Delta outflow	−0.28	0.1083	−0.18	0.1405
Average X2	0.29	0.0863	0.24	0.0494
Average LSZ area	−0.54	0.001	−0.41	0.0005
% days LSZ area > 75 km^2	−0.59	0.0002	− 0.44	0.0004

coarse-grid simulations, the entire vertical salinity profile is saved every 15 minutes at identical points spaced at 1-km intervals along the axis of the estuary. The position of X2 is then calculated at the end of each day by interpolating between the daily-averaged near bed salinity at each point to estimate the exact daily-averaged position of X2. Since the same points along the axis of the estuary are used for both calculations, and the accuracy of both models for predicting salinity is comparable (Table 3), the calculation of X2 is largely grid independent. In contrast, the LSZ area is calculated as the sum of the area of each grid cell where the daily-averaged depth-averaged salinity is between 0.5 and 6.0 psu. In the coarse-grid model, the largest cells in Grizzly Bay have an area greater than 1 km^2, and thus very small differences in salinity (6.01 psu vs 5.97 psu) can result in a noticeable scatter in LSZ area if multiple large cells are affected. As Figure 9B shows, the largest difference in LSZ area between the two models tends to occur when X2 is rapidly increasing or decreasing, and there is a large change in LSZ area over a short time. However, despite this somewhat larger scatter in LSZ area the correlation is still very high ($r^2 = 0.951$), and the seasonal patterns are very similar (Figure 9B). In addition, the accurate or very accurate prediction of salinity observations from the long-term fish monitoring programs across all years (indicated by all years falling inside radius 0.5 on Figure 7) demonstrates that the coarse-grid model is suitable for evaluating the estuary-wide salinity distribution over longer time-periods than are computationally feasible using the high-resolution model.

The fast computational speed that is possible using the coarse-grid model provides significant advantages over the high-resolution model for certain types of applications, such as simulating long time-periods to evaluate salinity distributions and long-term trends (as was done in this study), for rapid-response simulations to evaluate the effects of levee failures, or to pre-screen a large number of scenarios. The coarse-grid model also has significant advantages for stochastic applications that require a large number of scenarios, or for applications that require simulations that span decades or longer to evaluate long-term climate-change scenarios, the fate of legacy contaminants in bed sediments, or morphologic change.

When detailed information about the velocity field across the channel or at junctions is needed, however, or the components of a project design need to be evaluated at a higher level of detail, a higher-resolution model is still preferable. Regardless of the grid resolution and whether or not subgrid bathymetry is used, the UnTRIM hydrodynamic model solves for the velocity field at each grid face in each vertical layer and therefore cannot resolve cross-stream variation when using only 1 cell across a channel (Figure 1B). In some applications, even the grid size used in the high-resolution UnTRIM Bay–Delta model (Figure 2A) is not sufficient. For example, to investigate secondary circulation and the hydrodynamics at channel junctions, Bever and MacWilliams (2016) incorporated an even higher-resolution grid of the northern Delta than was used in previous applications into the UnTRIM Bay–Delta model. Similarly, for applications using particle-tracking models, such as the FISH–PTM used to evaluate entrainment based on fish movements (e.g., Gross et al. 2010; Blake et al. 2014), a high-resolution model that resolves the details of the velocity field is needed to provide sufficient detail to evaluate complex fish behaviors.

http://dx.doi.org/10.15447/sfews.2016v14iss2art3

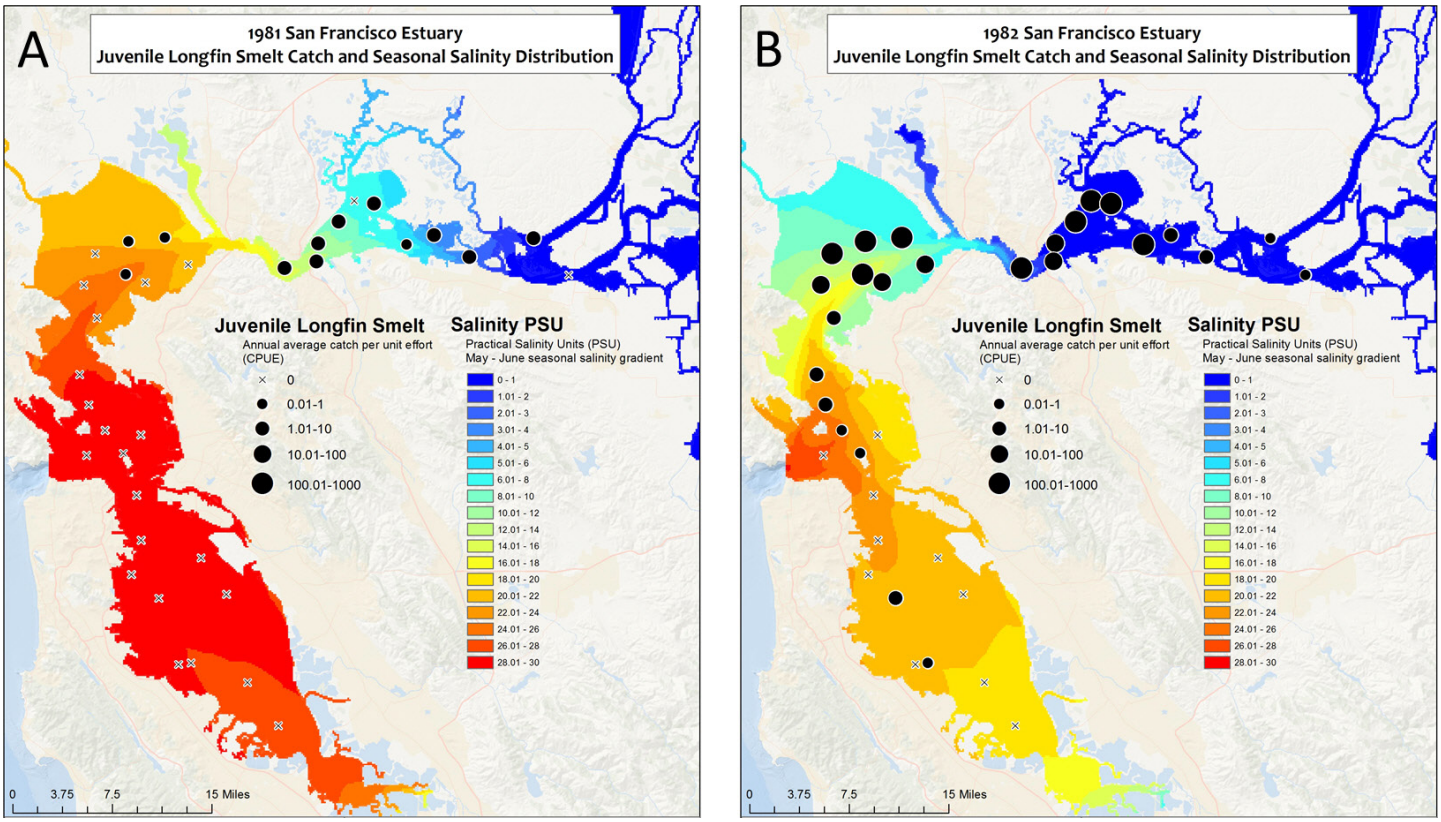

Figure 13 Predicted average salinity between May 1 and June 30 during **(A)** 1981 and **(B)** 1982 shown with the annual average CPUE of age–0 Longfin Smelt for each monitoring station in the San Francisco Bay Study midwater trawl

In any modeling application, there are trade-offs between grid resolution and computational speed such that a single model grid will never be suitable for all types of applications. This was also demonstrated by Irby et al. (2016) who compared eight hydrodynamic and dissolved oxygen models in the Chesapeake Bay and found that "when selecting the optimal resolution for a simulation, it is critical to weigh the advantages of increased resolution with the increased time required for simulation." The use of both a coarse-grid and a high-resolution model grid with the same hydrodynamic model and boundary conditions highlights the flexibility that can be achieved by using models of varying resolution over the same model domain to evaluate processes over multiple time-scales at different levels of detail.

Long-Term Trends in Salinity Distribution and LSZ Area

The 35-year time series of X2 and LSZ area (Figure 11) highlights the influence of multi-year climate patterns, shorter-duration weather, and Delta outflow on the salinity distribution within the estuary. While the area of the LSZ during the fall period between September 1 and November 30 is significantly influenced by hydrologic conditions, there has also been a long-term trend towards a smaller percentage of the time that the LSZ area exceeds 75 km^2 during the fall (Figure 12). Both the Spearman's rho and Kendall's tau rank correlations demonstrate significant trends of decreasing fall average LSZ area from 1980 to 2014, and a decreasing percentage of the time between September and November that the LSZ area is greater than 75 km^2 over this same time-period, despite the fact that both tests indicate there has not been a significant trend in fall average Delta outflow from

1980 through 2014. Though increasing fall salinity has been previously documented (e.g., Feyrer et al. 2007, 2011; Enright and Culberson 2009; Cloern and Jassby 2012), this analysis suggests that the trend of decreasing average LSZ area is not solely attributable to either increases in X2 or to decreases in outflow, since the trends for those variables are not as strong as for declining LSZ area. One potential explanation for this paradox may result from the non-monotonic relationship between X2 and LSZ area. Since the late 1990s, average Delta outflows between September and November have been trending towards an outflow that results in average X2 values between 80 and 90 km (Figure 12B). X2 values between 80 and 90 km correspond to a local minimum of LSZ area, because either higher or lower values of X2 result in an increase in the area of the LSZ (see Figure 12 in MacWilliams et al. 2015).

Salinity Field and Fish Abundance and Distribution

One of the goals of this study was to combine long-term fish monitoring data and hydrodynamic modeling results to improve communication among science, policy, and public audiences about how native and resident fish communities respond to changes in their estuarine habitat. The earliest CPUE maps in the estuary date back to the late-1940s (Erkkila et al. 1950). More recently, Sweetnam (1999) developed CPUE maps for Delta Smelt that demonstrated significant differences in the spatial distribution in Delta Smelt catch between wet and dry years (e.g., Figure 3 in Sweetnam 1999). The maps developed as part of this study build on these previous analyses by providing a more complete picture of the spatial distribution of salinity that corresponds to these different distributions in fish catch. Combining salinity distribution maps with CPUE data allows for a year-by-year assessment of the influence (or lack of influence) of salinity on fish distribution for different species. The full results of this study include 33 maps for each of six fishes (Table 2) that show variation in fish abundance and distribution simultaneously with seasonal variation in salinity distribution (EPA 2015). These maps illustrate the previously established relationships between salinity and abundance of fish populations (e.g., Jassby et al. 1995; Kimmerer 2002; Kimmerer et al. 2009), and allow for a visual assessment of how different fish species and life cycles respond to changes in estuarine salinity.

Although the traditional figures of abundance as a function of X2 (e.g., Jassby et al. 1995; Kimmerer et al. 2009) have some specific advantages for visualizing the relationship between abundance and habitat over a wide range of X2 on a single figure, the sequence of maps also has some benefits over the 1-D salinity metric X2 and the annual fish abundance index to communicate science to policy audiences. The maps show the full seasonal salinity distribution in two-dimensions, from seawater to freshwater, instead of a single number marking an average X2. The maps spatially display the distribution of individual fishes based on the annual average CPUE at each monitoring station so that changes in fish distribution and abundance can be observed visually. Finally, producing these maps for multiple species expands science and policy discussions beyond one fish, commonly Delta Smelt or Longfin Smelt, to include a larger estuarine community of fishes, which is more consistent with the CWA goal of protecting beneficial uses for aquatic life than focusing on individual species.

Applicability to Other Systems

A concern for multi-decadal hydrodynamic simulations is the lack of data available for model validation as simulation start dates recede in time. The model validation methods used in this study help to partially alleviate that concern by using a non-traditional data source to validate the predicted salinity distribution. The applicability of using point samples from fisheries survey data for model validation is not limited to the estuary. For example, at least two fisheries surveys are available in the Chesapeake Bay that could be used to validate model predictions. The Virginia Institute of Marine Science began monthly trawl sampling in 1955 (VIMS 2015) and the Maryland Department of Natural Resources began monthly trawl sampling in 1977 (MDNR 2015). Both these fisheries surveys have data before the 1984 start of the more traditional model validation data set collected by the Chesapeake Bay Program (EPA 2012b; CBP 2016).

In many long-term biological monitoring programs, such as the fisheries surveys noted above, the amount

http://dx.doi.org/10.15447/sfews.2016v14iss2art3

of data available to use to better understand the monitoring data and convey findings to stakeholders' decreases toward the beginning of the data sets. Although there is a similar limitation with decreasing data being available for model boundary conditions and calibration data, when sufficient model forcing data is available, detailed numerical models can provide data to interpret the biological monitoring data (Bever et al. 2016), both by filling-in information that was not collected at the time of the original surveys, and by helping visually convey the data sets themselves. The method presented in this paper for linking detailed salinity modeling with biological sampling to create a visual GIS is directly applicable to other systems. The resulting maps can be used to improve communication among stakeholders because they provide concise visual tools that convey the response of estuarine fishes to variation in their physical habitat (e.g., salinity, temperature, and dissolved oxygen). Presenting this information in a more easily understandable format facilitates a common understanding of scientific information that is essential for communicating estuarine management decisions to many diverse stakeholders.

CONCLUSIONS

The UnTRIM model was applied to San Francisco Bay and the Sacramento–San Joaquin Delta using a coarse resolution hydrodynamic model grid which used bathymetry represented at a finer subgrid scale. We simulated a 35-year period that spanned from January 1, 1980 through December 31, 2014. The model validation demonstrated that the coarse-grid model predicted water levels, flow, and salinity with accuracy comparable to the high-resolution UnTRIM Bay–Delta model (MacWilliams et al. 2015). We developed a method to validate the predicted spatial salinity distribution by comparing model predictions to surface salinity observations from long-term fish monitoring programs. This validation demonstrated that the coarse-grid UnTRIM Bay–Delta model predictions of the spatial surface salinity distribution from San Pablo Bay through the Delta were accurate or very accurate for all 33 years of the simulation (Figure 7). Taken together, the comparisons presented here demonstrate that the coarse-grid UnTRIM Bay–Delta model can predict the spatial distribution of the salinity field, X2, and LSZ area with sufficient accuracy throughout the simulation to provide reasonable salinity distribution maps dating back to at least 1980.

The 35-year period simulated for this study provides the opportunity to evaluate long-term trends in the area of the LSZ over a wide range of historic conditions. The 35-year time-series of predicted X2 and LSZ area highlight the influence of multiple-year climate patterns, shorter duration weather patterns, and Delta outflow on the salinity distribution within the estuary. The model predictions show generally less variability in the September through November average LSZ area after about 2000, with all 7 of the years with the lowest predicted average LSZ area between September and November occurring between 2000 and 2014.

Substantial advancements in GIS mapping and hydrodynamic modeling have occurred since scientists affiliated with the Interagency Ecological Program (IEP) devised the X2 approach for managing the LSZ in the estuary to protect fish. Our study used these advancements by creating a GIS framework that displays salinity distributions produced by the coarse-grid version of the 3-D UnTRIM San Francisco Bay–Delta model and long-term fish monitoring data from IEP's San Francisco Bay Study. The resulting maps can be used to improve communication among stakeholders because they depict the response of estuarine fishes to salinity conditions along the full salinity distribution from seawater to freshwater, rather than limiting discussion to a single fish species or focusing on a single salinity isohaline to represent the LSZ. In addition, the maps illustrate that it is feasible to use GIS to connect advancements in hydrodynamic models to biological monitoring to support and expand the array of scientific tools used to inform management decisions in the estuary. This type of analysis can be used to evaluate updates to salinity-based estuarine standards that are protective of water quality and aquatic life beneficial uses based on the best science available.

ACKNOWLEDGEMENTS

This project was conducted for the U.S. Environmental Protection Agency (EPA) Region 9 under subcontract to Tetra Tech, Inc (EP-G139-00187). Erin Foresman served as the technical

contact for the EPA. Jon Ludwig and Mustafa Faizullabhoy served as the technical contacts for Tetra Tech, Inc, and Amy King served as the contract manager. The UnTRIM code was developed by Professor Vincenzo Casulli (University of Trento, Italy). We would like to thank Dave Schoellhamer, Matt Nobriga, and an anonymous reviewer for their review comments and suggestions for improving this paper.

REFERENCES

Armor C, Herrgesell PL. 1985. Distribution and abundance of fishes in the San Francisco Bay estuary between 1980 and 1982. Hydrobiologia 129(1):211–227. doi: *http://dx.doi.org/10.1007/BF00048696*

Baxter R, Weib K, DeLeon S, Fleming K, Orsi J. 1999. Report on the 1980–1995 fish, shrimp, and crab sampling in the San Francisco Estuary, California. California Department of Fish and Game, Technical Report 63. Sacramento (CA): California Department of Water Resources. [accessed 2016 Jun 17]. *http://www.water.ca.gov/iep/docs/tech_rpts/tech_rprt_63_toc.html*

Bever AJ, MacWilliams ML, 2013. Simulating sediment transport processes in San Pablo Bay using coupled hydrodynamic, wave, and sediment transport models. Mar Geol 345:235–253. doi: *http://dx.doi.org/10.1016/j.margeo.2013.06.012*

Bever AJ, MacWilliams ML. 2016. Factors influencing the calculation of periodic secondary circulation in a tidal river: numerical modeling of the lower Sacramento River, USA. Hydrol Process 30(7):995–1016. doi: *http://dx.doi.org/10.1002/hyp.10690*

Bever AJ, MacWilliams ML, Wu F, Andes L, Conner CS. 2014. Numerical modeling of sediment dispersal following dredged material placements to examine the possible augmentation of the sediment supply to marshes and mudflats, San Francisco Bay, USA. Proceedings of the PIANC World Congress 2014; 2016 Jun 01–05; San Francisco, California. 18 p.

Bever AJ, MacWilliams ML, Herbold B, Brown LR, Feyrer FV. 2016. Linking hydrodynamic complexity to Delta Smelt (*Hypomesus transpacificus*) distribution in the San Francisco Estuary, USA. San Franc Estuary Watershed Sci 14(1). doi: *http://dx.doi.org/10.15447/sfews.2016v14iss1art3*

Blake A, Gross ES, Burau J, Saenz, B, Bever AJ, MacWilliams ML. 2014. Using individual based modeling to predict the distribution of juvenile salmon out-migrants in a reach of the Sacramento River. Prepared for the U.S. Bureau of Reclamation.

[CDEC] California Data Exchange Center. 2015. Chronological reconstructed Sacramento and San Joaquin Valley water year hydrologic classification indices. [accessed 2015 Aug 27]. *http://cdec.water.ca.gov/cgi-progs/iodir/wsihist*

[CDFW] California Department of Fish and Wildlife. 2015. Fall midwater trawl. [accessed 2015 Aug 27]. *https://www.dfg.ca.gov/delta/projects.asp?ProjectID=FMWT*

[CDWR] California Department of Water Resources. 2013. Dayflow, an estimate of daily average Delta outflow. [accessed 2013 Nov 07]. *http://www.water.ca.gov/dayflow/*

Casulli V. 1999. A semi-implicit numerical method for non-hydrostatic free-surface flows on unstructured grid. Numerical Modelling of Hydrodynamic Systems, ESF Workshop; 1999 Jun 21–24; Zaragoza, Spain. Zaragoza, Spain: University of Zaragoza. p. 175–193.

Casulli V. 2009. A high-resolution wetting and drying algorithm for free surface hydrodynamics. Int J Numer Meth Fl 60(4):391–408. doi: *http://dx.doi.org/10.1002/fld.1896*

Casulli V, Stelling G 2010. Semi-implicit subgrid modelling of three-dimensional free-surface flows. Int J Numer Meth Fl 67:441–449. doi: *http://dx.doi.org/10.1002/fld.2361*

Casulli V, Walters RA. 2000. An unstructured, three-dimensional model based on the shallow water equations. Int J Numer Meth Fl 32(3):331–348. doi: *http://onlinelibrary.wiley.com/doi/10.1002/(SICI)1097-0363(20000215)32:3%3C331::AID-FLD941%3E3.0.CO;2-C/abstract;jsessionid=40735E5222E3E76408AB321BCCCA605E.f03t04*

Casulli V, Zanolli P. 2002. Semi-implicit numerical modelling of non-hydrostatic free-surface flows for environmental problems. Math Comput Model 36(9–10):1131–1149. doi: *http://dx.doi.org/10.1016/S0895-7177(02)00264-9*

Casulli V, Zanolli P. 2005. High resolution methods for multidimensional advection-diffusion problems in free-surface hydrodynamics. Ocean Model 10(1–2):137–151. doi: *http://dx.doi.org/10.1016/j.ocemod.2004.06.007*

http://dx.doi.org/10.15447/sfews.2016v14iss2art3

[CBP] Chesapeake Bay Program. 2016. CBP water quality database, 1984–present. [accessed 2016 Jan 12]. Available from: *http://www.chesapeakebay.net/data/downloads/cbp_water_quality_database_1984_present*

Chua VP, Fringer OB. 2011. Sensitivity analysis of three-dimensional salinity simulations in the North San Francisco Bay using the unstructured-grid SUNTANS model. Ocean Model 39:332–350. doi: *http://dx.doi.org/10.1016/j.ocemod.2011.05.007*

Cloern JE, Jassby AD. 2012. Drivers of change in estuarine-coastal ecosystems: discoveries from four decades of study in San Francisco Bay. Rev of Geophys 50:RG4001. doi: *http://dx.doi.org/10.1029/2012RG000397*

Enright C, Culberson S. 2009. Salinity trends, variability, and control in the northern reach of the San Francisco Estuary. San Franc Estuary Watershed Sci 7(2). doi: *http://dx.doi.org/10.15447/sfews.2009v7iss2art3*

[EPA] U.S. Environmental Protection Agency. 2012a. Water quality challenges in the San Francisco Bay/Sacramento–San Joaquin Delta estuary: EPA's action plan. [accessed 2016 Jun 17]. *https://www.epa.gov/sites/production/files/documents/actionplan.pdf*

[EPA] U.S. Environmental Protection Agency. 2012b. Guide to using Chesapeake Bay Program Water Quality Monitoring Data, EPA 903-R-12-001. Annapolis (MD): U.S. Environmental Protection Agency Chesapeake Bay Program.

[EPA] U.S. Environmental Protection Agency. 2015. Salinity field and fish abundance and distribution visualization in the San Francisco Estuary. [accessed 2015 Oct 07]. *http://www2.epa.gov/sfbay-delta/fish-and-salinity-san-francisco-estuary*

Erkkila LF, Moffet JW, Cope OB, Smith BR, Nelson RS. 1950. Sacramento–San Joaquin Delta fishery resources: effects of Tracy Pumping Plant and the Delta Cross Channel. U.S. Fish and Wildlife Service Special Scientific Report 56. Washington, D.C.: U.S. Fish and Wildlife Service. 109 p.

Feyrer, F, Sommer, T, Hobbs, J. 2007. Living in a dynamic environment: variability in life history traits of age–0 splittail in tributaries of San Francisco Bay. Trans Am Fish Soc 136(5):1393–1405. doi: *http://dx.doi.org/10.1577/T06-253.1*

Feyrer F, Newman K, Nobriga M, Sommer T. 2011. Modeling the effects of future outflow on the abiotic habitat of an imperiled estuarine fish. Estuaries Coasts 34:120–128. doi: *http://dx.doi.org/10.1007/s12237-010-9343-9*

Gross ES, MacWilliams ML, Holleman CD, and Hervier TA. 2010. POD 3-D particle tracking modeling study, particle tracking model testing and applications report. [accessed 2016 Jun 17]. *http://www.science.calwater.ca.gov/pdf/workshops/POD/GrossEtAl_POD3D_Particle_tracking_2010.pdf*

Hofmann EE, Cahill B, Fennel K, Friedrichs MAM, Hyde K, Lee C, Mannino A, Najjar RG, O'Reilly JE, Wilkin J, et al. 2011. Modeling the dynamics of continental shelf carbon. Annu Rev Mar Sci 3:93–122. doi: *http://dx.doi.org/10.1146/annurev-marine-120709-142740*

Irby ID, Friedrichs MAM, Friedrichs CT, Bever AJ, Hood RR, Lanerolle LWJ, Scully ME, Sellner K, Shen J, Testa J, Wang H, Wang P, Linker L, Xia M. 2016. Challenges associated with modeling low-oxygen waters in Chesapeake Bay: a multiple model comparison. Biogeosciences 13:2011–2028. doi: *http://dx.doi.org/10.5194/bgd-12-20361-2015*

Jassby AD, Kimmerer WJ, Monismith SG, Armor C, Cloern JE, Powell TM, Schubel JR, Vendlinski TJ. 1995. Isohaline position as a habitat indicator for estuarine populations. Ecol Appl 5(1):272–289. doi: *http://dx.doi.org/10.2307/1942069*

Jolliff JK, Kindle JC, Shulman I, Penta B, Friedrichs MAM, Helber R, Arnone RA. 2009. Summary diagrams for coupled hydrodynamic-ecosystem model skill assessment. J Mar Syst. 76(1–2):64–82. doi: *http://dx.doi.org/10.1016/j.jmarsys.2008.05.014*

Kimmerer, W. 2002. Effects of freshwater flow on abundance of estuarine organisms: physical effects or trophic linkages? Mar Ecol Prog Ser 243:39–55. doi: *http://dx.doi.org/10.3354/meps243039*

Kimmerer WJ, Gross ES, MacWilliams ML. 2009. Is the response of estuarine nekton to freshwater flow in the San Francisco Estuary explained by variation in habitat volume? Estuar Coasts 32(2):375–389. doi: *http://dx.doi.org/10.1007/s12237-008-9124-x*

Lanerolle LW, Patchen RC, Aikman F. 2009. The second generation Chesapeake Bay Operational Forecast System (CBOFS2): a ROMS-based modeling system. In: 11th International Conference on Estuarine and Coastal Modeling, American Society of Civil Engineers, [2009 Nov 04–06]; Seattle, Washington. p 621-642. doi: *http://dx.doi.org/10.1061/41121(388)37*

Lanerolle LW, Patchen RC, Aikman F. 2011. The second generation Chesapeake Bay Operational Forecast System (CBOFS2): model development and skill assessment, report. Silver Spring (MD): U.S. Dept. of Commerce, National Oceanic and Atmospheric Administration, National Ocean Service, Office of Coast Survey, Coast Survey Development Laboratory. 77 p.

MacWilliams ML, Cheng RT. 2007. Three-dimensional hydrodynamic modeling of San Pablo Bay on an unstructured grid. Proceedings of the 7th International Conference on Hydroscience and Engineering (ICHE-2006); 2006 Sep 10–13; Philadelphia, PA. Philadelphia (PA): Drexel University. 16 p.

MacWilliams ML, Gross ES. 2007. UnTRIM San Francisco Bay–Delta Model calibration report, Delta Risk Management Study. Prepared for the California Department of Water Resources. 101 p.

MacWilliams ML, Gross ES, DeGeorge JF, Rachiele RR, 2007. Three-dimensional hydrodynamic modeling of the San Francisco Estuary on an unstructured grid. Proceedings of IAHR 32nd Congress; 2007 July 1–6; Venice Italy. 11 p.

MacWilliams ML, Salcedo FG, Gross ES. 2008. San Francisco Bay–Delta UnTRIM Model calibration report, POD 3-D Particle Tracking Modeling Study. Prepared for the California Department of Water Resources. 344 p.

MacWilliams ML, Salcedo FG, Gross ES. 2009. San Francisco Bay–Delta UnTRIM Model Calibration Report, Sacramento and Stockton Deep Water Ship Channel 3-D Hydrodynamic and Salinity Modeling Study. Prepared for U.S. Army Corps of Engineers, San Francisco District. 574 p.

MacWilliams ML, Gross ES. 2013. Hydrodynamic simulation of circulation and residence time in Clifton Court Forebay. San Franc Estuary Watershed Sci 11(2). doi: *http://dx.doi.org/10.15447/sfews.2013v11iss2art1*

MacWilliams ML, Sing PF, Wu F, Hedgecock N. 2014. Evaluation of the potential salinity impacts resulting from the deepening of the San Francisco Bay to Stockton Navigation Improvement Project. In: Proceedings of 33rd PIANC World Congress; 2014 Jun 01–05; San Francisco, CA. 13 p.

MacWilliams ML, Bever AJ, Gross ES, Ketefian GA, Kimmerer WJ. 2015. Three-dimensional modeling of hydrodynamics and salinity in the San Francisco Estuary: an evaluation of model accuracy, X2, and the low salinity zone. San Franc Estuary Watershed Sci 13(1). doi: *http://dx.doi.org/10.15447/sfews.2015v13iss1art2*

[MDNR] Maryland Department of Natural Resource. 2015. 2012 blue crab summer trawl survey. [accessed 2015 Oct 07]. *http://dnr2.maryland.gov/fisheries/Pages/blue-crab/trawl.aspx*

Moyle PB, Herbold B, Stevens DE, Miller LW. 1992. Life history and status of Delta Smelt in the Sacramento–San Joaquin Estuary, California. Trans Am Fish Soc 121:67–77. doi: *http://www.tandfonline.com/doi/abs/10.1577/1548-8659%281992%29121%3C0067%3ALHASOD%3E2.3.CO%3B2*

Rosenfield JA, Baxter RD. 2007. Population dynamics and distribution patterns of Longfin Smelt in the San Francisco Estuary. Trans Am Fish Soc 136(6):1577–1592. doi: *http://dx.doi.org/10.1577/T06-148.1*

Song H, Miller AJ, McClatchie S, Weber ED, Nieto KM, Checkley Jr. DM. 2012. Application of a data-assimilation model to variability of Pacific Sardine spawning and survivor habitats with ENSO in the California Current System. J Geophys Res Oceans 17:C03009. doi: *http://dx.doi.org/10.1029/2011JC007302*

Stevens DE, Miller LW. 1983. Effects of river flow on abundance of young Chinook salmon, American shad, longfin smelt, and delta smelt in the Sacramento–San Joaquin River system. N Am J fish Manage 3(4):425–437.

Sehili A, Lang G, Lippert C. 2014. High-resolution subgrid models: background, grid generation, and implementation. Ocean Dyn 64(4):519–535. doi: *http://dx.doi.org/10.1007/s10236-014-0693-x*

http://dx.doi.org/10.15447/sfews.2016v14iss2art3

Sweetnam DA. 1999. Status of Delta Smelt in the Sacramento–San Joaquin Estuary. Calif Fish Game 85(1):22–27.

Turner JL, Chadwick HK. 1972. Distribution and abundance of young-of-the-year striped bass, *Morone saxatilis*, in relation to river flow in the Sacramento–San Joaquin Estuary. Trans Am Fish Soc 101(3):442–452.

[VIMS] Virginia Institute of Marine Science. 2015. Juvenile fish and blue crab trawl survey [Internet]. [cited 07 Oct 2015]. Available from: *http://www.vims.edu/research/departments/fisheries/programs/juvenile_surveys/index.php*

Willmott CJ. 1981. On the validation of models. Phys Geogr 2:184–194. doi: *http://www.tandfonline.com/doi/abs/10.1080/02723646.1981.10642213*

Xu J, Long W, Wiggert JD, Lanerolle LW, Brown CW, Murtugudde R, Hood RR. 2012. Climate forcing and salinity variability in Chesapeake Bay, USA. Estuaries Coasts. 35(1):237–261. doi: *http://dx.doi.org/10.1007/s12237-011-9423-5*

ADDITIONAL REFERENCES

Lippert C. 2009. Grid generation for UnTRIM^2 with special respect to sub-grid generation. In: 6th International UnTRIM Workshop; 2009 May 11–13; Trento, Italy. 35 p.